 

PACS numbers: 78.60.Fi; 78.66.Hf; 85.60.Jb
DOI: 10.1070/QE2011v041n01ABEH014421

# Electroluminescence of ZnO-based semiconductor heterostructures

O.A. Novodvorsky, A.A. Lotin, V.Ya. Panchenko, L.S. Parshina, E.V. Khaidukov, D.A. Zuev, O.D. Khramova

***Abstract*. Using pulsed laser deposition, we have grown n-ZnO/p-GaN, n-ZnO/i-ZnO/p-GaN and n-ZnO/n-$Mg_{0.2}Zn_{0.8}O$/i-$Cd_{0.2}Zn_{0.8}O$/p-GaN light-emitting diode (LED) heterostructures with peak emission wavelengths of 495, 382 and 465 nm and threshold current densities (used in electroluminescence measurements) of 1.35, 2, and 0.48 A $cm^{-2}$, respectively. Because of the spatial carrier confinement, the n-ZnO/n-$Mg_{0.2}Zn_{0.8}O$/i-$Cd_{0.2}Zn_{0.8}O$/p-GaN double heterostructure LED offers a higher electroluminescence intensity and lower electroluminescence threshold in comparison with the n-ZnO/p-GaN and n-ZnO/i-ZnO/p-GaN LEDs.**

***Keywords***: *pulsed laser deposition, zinc oxide, light-emitting heterostructures.*

## 1. Introduction

The unabated interest in the problem of creating various ZnO-based semiconductor devices stems from the wide range of unique properties offered by this material. Zinc oxide, a direct-gap semiconductor with a band gap $E_g = 3.37$ eV, is a candidate material for near-UV light-emitting diodes (LEDs). It has the highest exciton binding energy among semiconductors (60 meV), which allows ZnO-based devices to operate at temperatures of up to 700 °C [1]. Since zinc oxide possesses high chemical stability and radiation hardness, it can be used in nuclear and space applications [2].

Because of the deviations from stoichiometry due to native point defects associated with a certain degree of disorder, which corresponds to the equilibrium state of the crystal, with the lowest possible Gibbs free energy, even undoped zinc oxide is n-type. Pulsed pulsed laser deposition is successfully used to produce high-quality epitaxial ZnO films [3]. Zinc oxide films doped with Group III elements during the deposition process have high n-type conductivity stable in time and good structural perfection [4, 5]. Much more serious difficulties are encountered in producing p-type ZnO films [6 – 9]. Despite the large number of reports on the growth of p-type ZnO films, only a few studies have been concentrated on the fabrication of ZnO-based LEDs [10, 11]. To obviate the problem of producing p-type ZnO films, a number of researchers employed semiconductors such as SiC [12], GaN [13] and even Si [14] as hole injectors.

In this paper, we report the growth of n-ZnO/p-GaN, n-ZnO/i-ZnO/p-GaN and n-ZnO/n-$Mg_{0.2}Zn_{0.8}O$/i-$Cd_{0.2}Zn_{0.8}O$/p-GaN light-emitting heterostructures on p-GaN films by pulsed laser deposition and their optical and electrical properties.

**O.A. Novodvorsky, A.A. Lotin, V.Ya. Panchenko, L.S. Parshina, E.V. Khaidukov, D.A. Zuev, O.D. Khramova** Institute on Laser and Information Technologies, Russian Academy of Sciences, Svyatoozerskaya ul. 1, 140700 Shatura, Moscow region, Russia; e-mail: onov@mail.ru

Received 22 September 2010
*Kvantovaya Elektronika* **41** (1) 4 – 7 (2011)
Translated by O.M. Tsarev

## 2. Experimental

Our experiments involved several steps. First, a GaN buffer layer $\sim 3$ μm in thickness was grown by MOCVD on a (0001) sapphire substrate in order to compensate dislocations due to the lattice mismatch between sapphire and gallium nitride. Then, a ca. 500-nm-thick Mg-doped (0.1 at %) p-GaN film was grown on the buffer. Hall effect measurements showed that the hole concentration in the p-GaN film was $8.8 \times 10^{17}$ $cm^{-3}$ and the hole mobility was $\mu = 14.3$ $cm^2$ $V^{-1}$ $s^{-1}$. The resistivity of the film, $\rho_p$, was 0.86 Ω cm.

Next, three different mesa structures $400 \times 400$ μm in lateral dimensions were grown on the p-GaN film by pulsed laser deposition: n-type ZnO : Ga film (400 nm thick); n-type ZnO : Ga film with an intermediate undoped zinc oxide layer, n-ZnO(400 nm)/i-ZnO(50 nm); and an n-ZnO(400 nm)/n-$Mg_{0.2}Zn_{0.8}O$(200 nm)/i-$Cd_{0.2}Zn_{0.8}O$(200 nm) double heterostructure (Fig. 1a). The mesa structures were produced using silicon masks fabricated by plasma etching. Targets were ablated by the radiation from an LC-7020 excimer laser pulsed at a repetition rate of 10 Hz ($\lambda = 248$ nm, $\tau = 15$ ns). The laser energy density delivered to the target surface was 4 J $cm^{-2}$. During the ablation process, the deposition temperature was maintained at 450 °C, and the $O_2$ buffer gas pressure in the ablation chamber was 10 mTorr. Electronic conduction in the n-ZnO and n-$Mg_{0.2}Zn_{0.8}O$ films was ensured by gallium doping to 0.25 at %. The resistivity of the n-ZnO film, $\rho_n$, was $1 \times 10^{-3}$ Ω cm. Ohmic contacts to the n-ZnO epitaxial film were made from Au/Ni, and those to the p-GaN film, from Pt. The contacts were annealed at 700 °C.

To study the structural and optical properties of the heterostructures, we grew and investigated gallium-doped (0.25 at %) n-ZnO and n-$Mg_{0.2}Zn_{0.8}O$ films and an undoped

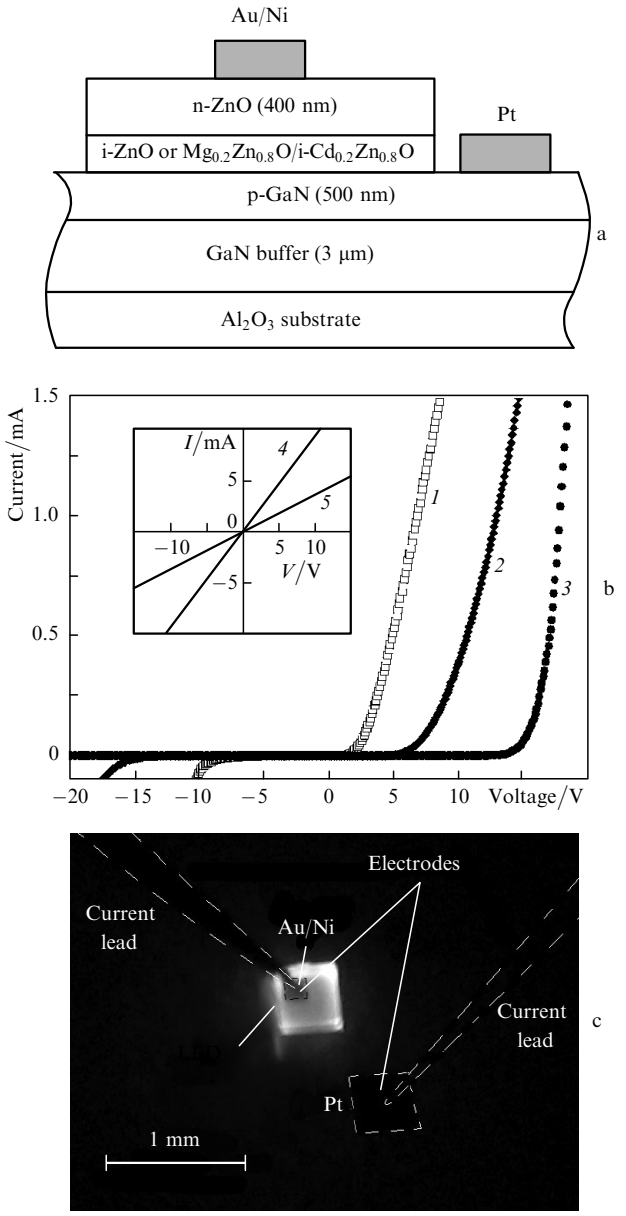


**Figure 1.** (a) Schematic of the LED structure. (b) Current–voltage curves of the (*1*) n-ZnO/p-GaN, (*2*) n-ZnO/i-ZnO/p-GaN and (*3*) n-ZnO/n-$Mg_{0.2}Zn_{0.8}O$/i-$Cd_{0.2}Zn_{0.8}O$/p-GaN LEDs and the Ohmic contacts to the (*4*) n-ZnO and (*5*) p-GaN films (inset). (c) Photograph of the n-ZnO/p-GaN heterostructure, which electroluminesces under forward bias at a current density $J = 30$ A cm$^{-2}$.

$Cd_{0.2}Zn_{0.8}O$ film 200 nm in thickness on sapphire substrates. Their structure was examined on a Bruker AXS D8 Discover all-purpose X-ray diffractometer in parallel beam geometry. To study the optical properties of the films, we measured their transmission spectra, $T(\lambda)$, using a Varian Cary-50 spectrophotometer, and their photoluminescence spectra, $I_{PL}(\lambda)$, at room temperature. The photoluminescence of the films was excited by a 20-mW 325-nm cw He–Cd laser beam (NPO Plazma, Russia). Their photo- and electroluminescence spectra were taken on an Ocean Optics HR4000 spectrometer. The resistivity of the films was determined by four-point probe van der Pauw measurements using a Lucas Labs Pro4 system. The current–voltage characteristics of the LEDs and Ohmic contacts were measured with a Keithley 2612 voltmeter equipped with a built-in pulsed power supply.

## 3. Experimental results and discussion

X-ray diffraction measurements showed that the in-plane lattice mismatch $\Delta a/a$ in the n-ZnO/n-$Mg_{0.2}Zn_{0.8}O$ and n-$Mg_{0.2}Zn_{0.8}O$/i-$Cd_{0.2}Zn_{0.8}O$ heterojunctions was within 0.5 %. The lattice mismatch in the n-ZnO/p-GaN and i-$Cd_{0.2}Zn_{0.8}O$/p-GaN heterojunctions was 0.66 % and 2.26 %, respectively.

Figure 1 shows a schematic of the LED heterostructures and the current–voltage curves of the n-ZnO/p-GaN, n-ZnO/i-ZnO/p-GaN and n-ZnO/n-$Mg_{0.2}Zn_{0.8}O$/i-$Cd_{0.2}Zn_{0.8}O$/ p-GaN diode heterostructures. The curves exhibit well-defined rectifying behaviour. The forward threshold voltage of the n-ZnO/p-GaN and n-ZnO/i-ZnO/p-GaN diodes is 3.1 and 9.5 eV, and their peak reverse voltage is 10.5 and 16.5 V, respectively. The forward threshold voltage $V_{th}$ of the n-ZnO/n-$Mg_{0.2}Zn_{0.8}O$/i-$Cd_{0.2}Zn_{0.8}O$/p-GaN double heterostructure LED is the highest, 16.3 V, and its peak reverse voltage exceeds 20 V. The larger number of interfaces and, hence, of barriers to charge carriers and the rather large lattice mismatch between the i-$Cd_{0.2}Zn_{0.8}O$ and p-GaN films increase $V_{th}$. Moreover, these factors underlie the locking of charge carriers of opposite signs, increasing the peak reverse voltage.

It is known that p-type semiconductors form Ohmic contacts with metals whose work function $\Phi_m$ exceeds the sum of the electron affinity $\chi_s$ and band gap $E_g$ of the semiconductor [15]:

$$\Phi_m > E_g + \chi_s.$$

However, in the case of wide-gap semiconductors, including GaN ($E_g = 3.39$ eV, $\chi_s = 4.1$ eV), there are no metals with a work function exceeding the sum $E_g + \chi_s$. Our results indicate that only platinum, with the highest work function ($\Phi_m = 5.65$ eV) among metals, ensures Ohmic contacts to p-GaN films. The inset in Fig. 1b shows the current–voltage curves of the Au/Ni and Pt Ohmic contacts to the n-ZnO and p-GaN films, respectively.

Figure 1c is a photograph of the electroluminescent n-ZnO/p-GaN heterostructure, and Fig. 2a shows the electroluminescence spectra, $I_{EL}(\lambda)$, of the n-ZnO/p-GaN, n-ZnO/i-ZnO/p-GaN and n-ZnO/n-$Mg_{0.2}Zn_{0.8}O$/i-$Cd_{0.2}Zn_{0.8}O$/p-GaN heterostructures. It can be seen that the luminescence of the p–n heterojunctions is brighter on their periphery than in their central part. The likely reason for this is that the use of a silicon mask leads to inhomogeneities in the depth direction near the edge of the mask, which in turn increases the electric field strength in the peripheral part of the mesa structure relative to that in the planar part of the p–n heterojunction. Therefore, carrier recombination will take place predominantly at the edge of the structure [16]. Lithography would ensure uniform emission from the entire surface.

We examined the effect of pump current density $J$ on the electroluminescence intensity $I_{EL}$. The results are presented in Fig. 2b. The 495-nm $I_{EL}$ of the n-ZnO/p-GaN LED increases linearly up to $J = 30$ A cm$^{-2}$. At higher current densities, the curve has a lower slope. The threshold current density for electroluminescence in the n-ZnO/p-GaN diode

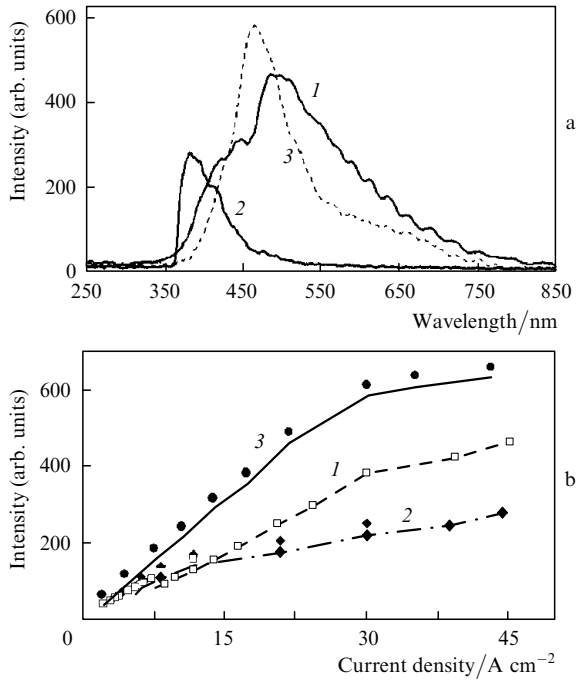


**Figure 2.** (a) Electroluminescence spectra at a current density $J = 30$ A cm$^{-2}$ and (b) electroluminescence intensity vs. current density for the (*1*) n-ZnO/p-GaN, (*2*) n-ZnO/i-ZnO/p-GaN and n-ZnO/n-$Mg_{0.2}Zn_{0.8}O$/i-$Cd_{0.2}Zn_{0.8}O$/p-GaN LEDs.

is $J_{th} = 1.35$ A cm$^{-2}$. The peak emission wavelength of the n-ZnO/i-ZnO/p-GaN LED is 382 nm (Fig. 2a), and its threshold current density is 2 A cm$^{-2}$. Despite the high forward threshold voltage of the n-ZnO/n-$Mg_{0.2}Zn_{0.8}O$/i-$Cd_{0.2}Zn_{0.8}O$/p-GaN LED, its threshold current density

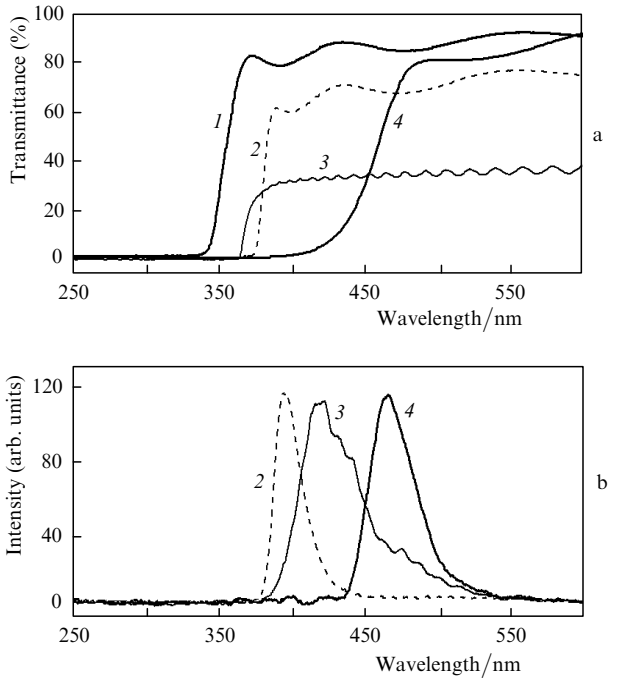


**Figure 3.** (a) Transmission and (b) photoluminescence spectra of the (*1*) n-$Mg_{0.2}Zn_{0.8}O$, (*2*) n-ZnO, (*3*) p-GaN and (*4*) i-$Cd_{0.2}Zn_{0.8}O$ films.

**Table 1.** Lattice parameter $a$, band gap $E_g$, electron affinity $\chi_s$ and resistivity $\rho$ of the ZnO, n-ZnO, i-$Cd_{0.2}Zn_{0.8}O$, n-$Mg_{0.2}Zn_{0.8}O$ and p-GaN films.

| Film | $a$/Å | $E_g$/eV | $\chi_s$/eV | $\rho$/Ω cm |
|---|---|---|---|---|
| ZnO | 3.2506 | 3.3 | 4.3 | 4.9 |
| n-ZnO | 3.165 | 3.35 | 4.3 | $9.7 \times 10^{-4}$ |
| i-$Cd_{0.2}Zn_{0.8}O$ | 3.258 | 2.86 | 4.43 | 3.35 |
| n-$Mg_{0.2}Zn_{0.8}O$ | 3.241 | 3.62 | 3.78 | 0.24 |
| p-GaN | 3.186 | 3.39 | 4.1 | 0.86 |

is 0.48 A cm$^{-2}$. The lower $J_{th}$ is due to the higher quantum efficiency of the double heterostructure [17].

To locate the radiative recombination region, we measured the photoluminescence and transmission spectra of the n-ZnO, n-$Mg_{0.2}Zn_{0.8}O$, i-$Cd_{0.2}Zn_{0.8}O$ and p-GaN films. The results are presented in Fig. 3. From the transmission spectra, we evaluated the band gap $E_g$ of the films (Table 1).

Comparison of the photo- and electroluminescence spectra leads us to conclude that, in the n-ZnO/p-GaN

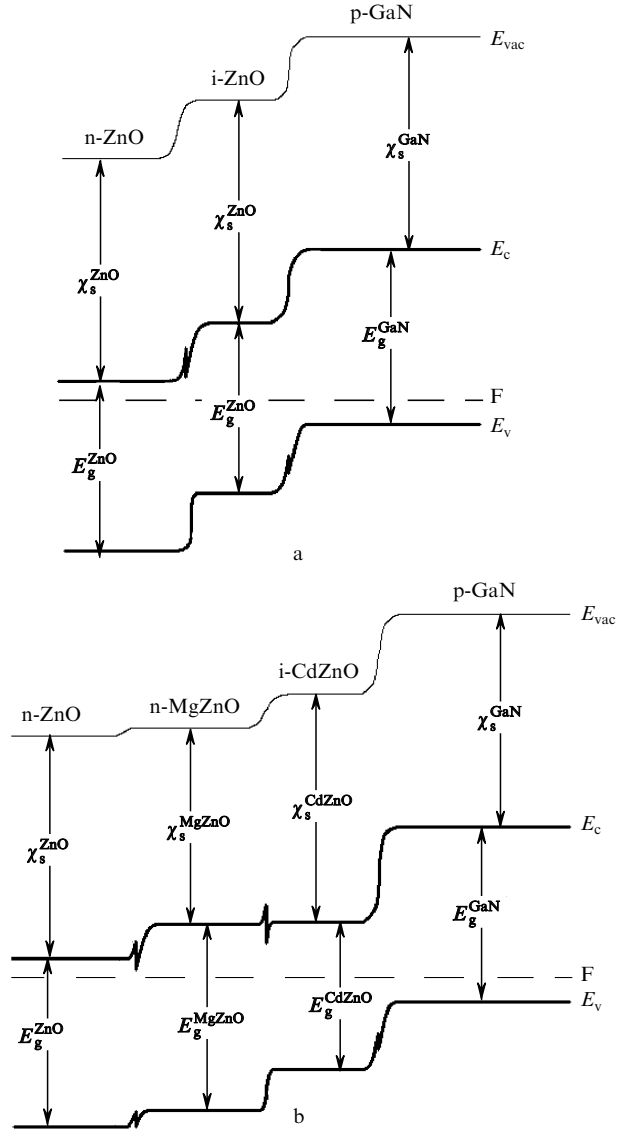


**Figure 4.** Energy band diagrams of the (a) n-ZnO/i-ZnO/p-GaN and (b) n-ZnO/n-$Mg_{0.2}Zn_{0.8}O$/i-$Cd_{0.2}Zn_{0.8}O$/p-GaN LED heterostructures: $E_{vac}$ is the vacuum level, $E_c$ is the conduction band bottom, $E_v$ is the valence band top, and F is the Fermi level.

LED, radiative electron – hole recombination takes place predominantly in the p-GaN layer. This is due to the higher electron mobility in the n-ZnO layer in comparison with the hole mobility in the p-GaN layer, which leads to faster electron diffusion to the p-layer in comparison with the hole diffusion to the n-ZnO layer [18]. Despite the large band gap of gallium nitride, radiative recombination in GaN-based LEDs is mainly due to native point defects that have deep energy levels in its band gap [19]. As shown by Kaiser et al. [20], the blue emission band centred at 2.8 eV in the photoluminescence spectrum of GaN films arises from donor – acceptor recombination where the donor is a nitrogen vacancy in one of its possible charge states.

Figure 4 shows the energy band diagrams of the n-ZnO/i-ZnO/p-GaN and n-ZnO/n-$Mg_{0.2}Zn_{0.8}O$/i-$Cd_{0.2}Zn_{0.8}O$/p-GaN LED heterostructures in the electron affinity model [16]. The electron affinities of the semiconductors involved are listed in Table 1. The i-ZnO undoped layer between the n- and p-layers enables a reduction in the barrier to holes (Fig. 4a) and injection of electrons and holes to the i-ZnO intermediate layer, where they recombine. As a result, the electroluminescence spectrum of the n-ZnO/i-ZnO/p-GaN LED shows a relatively narrow peak due to interband carrier recombination (Fig. 2a). The n-$Mg_{0.2}Zn_{0.8}O$ layer in the n-ZnO/n-$Mg_{0.2}Zn_{0.8}O$/i-$Cd_{0.2}Zn_{0.8}O$/p-GaN LED produces an extra barrier to electrons, preventing too rapid electron outflow to the p-GaN layer, and the i-$Cd_{0.2}Zn_{0.8}O$ narrow-gap layer reduces the barrier to holes to a greater extent than does the i-ZnO layer. Consequently, the carriers are fully locked in the i-$Cd_{0.2}Zn_{0.8}O$ layer, which acts as an active layer. That the electroluminescence spectrum of the diode coincides with the photoluminescence spectrum of the $Cd_{0.2}Zn_{0.8}O$ film confirms that carrier recombination occurs in the narrow-gap layer.

## 4. Conclusions

Using an i-$Cd_{0.2}Zn_{0.8}O$ narrow-gap layer, we have fabricated an n-ZnO/n-$Mg_{0.2}Zn_{0.8}O$/i-$Cd_{0.2}Zn_{0.8}O$/p-GaN double heterostructure LED which offers a higher electroluminescence intensity (due to spatial carrier confinement) and a lower electroluminescence threshold in comparison with n-ZnO/p-GaN and n-ZnO/i-ZnO/p-GaN LEDs. Varying the Cd content of the active layer, one will be able to produce blue and near-UV light sources.

***Acknowledgements.*** This work was supported by the Russian Foundation for Basic Research (Grant Nos 09-08-00291-a and 09-07-00208-a).

## References

1. Ozgur U., Alivov Ya.I., Liu C., Teke A., Reshchikov M.A., Dogan S., Avrutin V., Cho S.-J., Morkoc H. *J. Appl. Phys.*, **98**, 041301 (2005).
2. Look D.C., Reynolds D.C., Litton C.W., Jones R.L., Eason D.B., Cantwell G. *Appl. Phys. Lett.*, **81**, 1830 (2002).
3. Panchenko V.Ya., Novodvorsky O.A., Golubev V.S. *Nauka Tekhnol. Prom-sti*, (4), 39 (2006).
4. Panchenko V.Ya., Novodvorsky O.A., Golubev V.S. *Perspekt. Mater.*, **1**, 39 (2007).
5. Novodvorsky O.A., Gorbatenko L.S., Panchenko V.Ya., Khramova O.D., Cherebilo Ye.A., Wenzel C., Bartha J.W., Bublik V.T., Shcherbachev K.D. *Fiz. Tekh. Poluprovodn.*, **43**, 440 (2009).
6. Zhao J.-L., Li X.-M., Bian J.-M., Yu W.-D., Zhang C.-Y. *J. Cryst. Growth*, **280**, 495 (2005).
7. Rogozin I.V. *Fiz. Tekh. Poluprovodn.*, **43**, 26 (2009).
8. Ye Z., Wang J., Wu Ya., Zhou X., Chen F., Xu W., Miao Ya., Huang J., Lu J., Zhu L., Zhao B. *Front. Optoelectron. China*, **1**, 147 (2008).
9. Zhang J., Xue Sh., Shao L. *J. Semicond.*, **31**, 043001 (2010).
10. Tsukazaki A., Ohtomo A., Onuma T., Ohtani M., Makino T., Sumiya M., Ohtani K., Chichibu S.F., Fuke S., Segava Y., Ohno H., Koinuma H., Kawasaki M. *Nat. Mater.*, **4**, 42 (2005).
11. Ryu Y., Lee T.-S., Lubguban J.A., White H.W., Kim B.-J., Park Y.S., Youn C.J. *Appl. Phys. Lett.*, **88**, 241108 (2006).
12. Nakamura A., Ohashi T., Yamamoto K., Ishihara J., Aoki T., Temmio J., Gotoh H. *Appl. Phys. Lett.*, **90**, 093512 (2007).
13. Georgobiani A.N., Gruzintsev A.N., Vorob'ev M.O., Kaiser U., Richter W., Khodos I.I. *Fiz. Tekh. Poluprovodn.*, **35**, 725 (2001).
14. Tan S.T., Sun X.W., Zhao J.L., Iwan S., Cen Z.H., Chen T.P., Ye J.D., Lo G.Q., Kwong D.L., Teo K.L. *Appl. Phys. Lett.*, **93**, 013506 (2008).
15. Blank T.V., Gol'dberg Yu.A. *Fiz. Tekh. Poluprovodn.*, **41**, 1288 (2007).
16. Lebedev A.I. *Fizika poluprovodnikovykh priborov* (The Physics of Semiconductor Devices) (Moscow: Fizmatlit, 2008).
17. Alferov Zh.I. *Usp. Fiz. Nauk*, **172**, 1073 (2002).
18. Schubert E.F. *Light-Emitting Diodes* (Cambridge: Cambridge Univ. Press, 2006, 2nd ed.; Moscow: Fizmatlit, 2008).
19. Nakamura S., Iwasa N., Senoh M., Mukai T. *Jpn. J. Appl. Phys.*, **31**, 1258 (1992).
20. Kaiser U., Gruzintsev A.N., Khodos I.I., Richter W. *Neorg. Mater.*, **36** (6), 720 (2000).